NTRD Technical Monthly August FY18

Nuclear Technology Research and Development

Prepared for
U.S. Department of Energy

October 12, 2018

NTRD-PAC-2018-000479
INL/EXT-18-51702

CONTENTS

FIGURES

ADVANCED FUELS CAMPAIGN

MATERIAL RECOVERY AND WASTE FORMS DEVELOPMENT

NUCLEAR TECHNOLOGY RESEARCH AND DEVELOPMENT TECHNICAL MONTHLY AUGUST FY18

Advanced Fuels Campaign

ADVANCED LWR FUELS

LWR Fuels

- **[LANL]** A Level 3 milestone report titled, "Crystal Structure Evolution of U-Si Nuclear Fuel Phases as a Function of Temperature," was submitted by S. Vogel, J. White (both LANL) and T. Wilson (University of South Carolina, Columbia). The crystal structure of the U3Si2 line compound in the U-Si system was investigated as a function of temperature from room temperature to 1373 K using high temperature neutron time-of-flight diffraction on the HIPPO diffractometer at LANSCE. The U-Si system is actively researched due to its promise as an accident tolerant nuclear fuel. The simultaneous Rietveld refinement of five histograms from the five HIPPO detector rings provided fundamental datasets for the lattice parameters, anisotropic atomic displacement parameters, and atomic positions as a function of temperature. To explore the possibility of minority phases as a result of the synthesis route and especially due to hyper-stoichiometry, a stoichiometric U3Si2.00 sample and a hyper-stoichiometric U3Si2.01 sample were studied. While minor differences in the anisotropic atomic displacement parameters between the two samples were observed, over the entire investigated temperature range no additional phases were observed. However, significant differences in the thermal expansion behavior were identified between the two compositions that warrant future investigation. (K. McClellan)

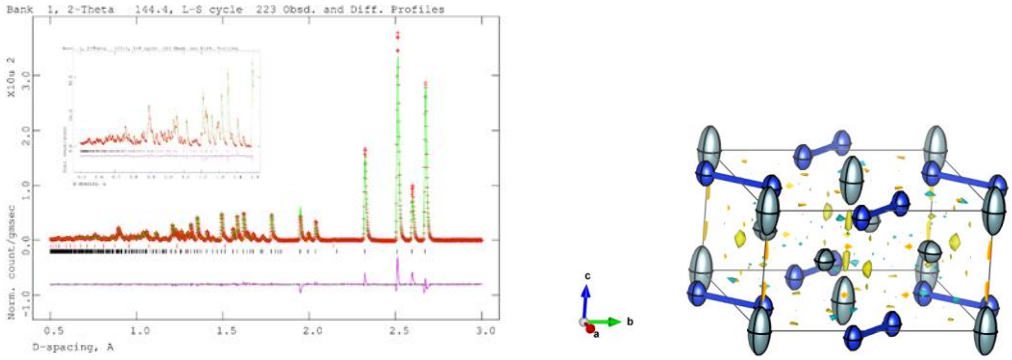

(a) (b)

Figure 1. a) Diffraction data (crosses) and Rietveld fit (curve) with difference curve (below) for a 12 hour long count time room temperature run with U3Si2.01 for the high resolution 145° HIPPO detectors. The inset shows the low d-spacing region. Tick marks indicate peak positions for U_3Si_2 (lower row) and the vanadium sample container. No other phases were detected for this hyper-stoichiometric sample. (b) Crystal structure of U_3Si_2 resulting from the Rietveld refinement of the data. The significant anisotropic thermal motion of the uranium atoms on the corners is evident as ellipsoidal atomic displacements. The second uranium (also silver colored) and the Si atom (blue color) exhibit a more isotropic atomic displacement.

- **[LANL]** The Level 3 milestone titled, "Mechanical properties of LWR fuel materials at elevated temperatures," was submitted by U. Carvajal-Nunez. Fundamental thermomechanical properties of U3Si2, CeO2, and UO2 were determined at elevated temperatures using resonant ultrasound spectroscopy (RUS). The elastic behavior of unirradiated nuclear fuels at high temperatures has only been explored to a limited extent using conventional mechanical testing techniques. In this study, the fundamental elastic properties of CeO2, UO2 and U3Si2 from room temperature up to 500 K were assessed using the RUS technique providing a novel methodology to determine thermoelastic behavior of nuclear fuel elements. (U. Carvajal-Nunez)
- **[ORNL]** The Level 2 milestone, M2NT-18OR020201051 titled, "Issue report on the development of a characterization methodology for separate effects testing of irradiated ceramic fuels," was completed. This consisted of development of a post-irradiation characterization methodology for the miniature (MiniFuel) project. The MiniFuel concept is currently being used for irradiation testing of small geometries of ceramic fuels in the High Flux Isotope Reactor (HFIR). This irradiation concept provides an efficient pipeline of currently existing and novel fuel types for separate effects screening and benchmarking prior to full-scale irradiation experiments. The work completed within the scope of the milestone involved the development of post-irradiation techniques including disassembly, specimen retrieval, fission gas release analysis and dimensional changes of the fuel. These methods have been demonstrated and are ready for in-cell implementation on the first set of irradiated MiniFuel specimens. A level two milestone is currently planned for FY19 to describe the results of disassembly and post-irradiation examination of these specimens using the established methodology. (A.M. Raftery, R.N. Morris, K.R. Smith, G.W. Helmreich, C.M. Petrie, K.A. Terrani, A.T. Nelson)

LWR Core Materials

- **[LANL]** Nanohardness testing was completed on a C26M FeCrAl weld and compared to previous testing on other FeCrAl welds. Results were summarized in a report to meet a Level 3 milestone. Results show the grain size distribution across the weld and heat affected zones and how it varies in the different materials. (S. Maloy)
- **[LANL]** Elevated temperature tensile testing was completed on FeCrAl alloys irradiated in HFIR. Results are being compiled in a report to meet the Level 3 milestone due next month. (T. Saleh)
- **[ORNL]** The Level 3 milestone M3NT-18OR020202073 titled, "Application of Binderjet Technology for Advanced Manufacturing of Ceramic Components," due on 8/16/2018 was successfully completed. The corresponding report documents a first of a kind demonstration for advanced manufacturing of a refractory ceramic, silicon carbide to produce components with complex geometry. The advanced manufacturing methodology results from a novel combination of binder jet printing with chemical vapor infiltration. Detailed processing methodology and the resulting material microstructure and properties are reported in this study. (K. Terrani, M. Trammell, B. Jolly, R. Seibert, F. Montgomery, H. Wang)
- **[LANL]** Oxides were characterized on FeCrAl alloys after exposure to steam. Data was summarized in a report to meet a Level 3 milestone. Results show the details of the very thin oxide produced under these conditions to provide protection from further oxidation. (T. Saleh)
- **[ORNL]** In August, the Level 2 Milestone M2NT-18OR020202091 titled, "Issue Update FeCrAl Cladding Handbook of Properties," was successfully completed. The revisions briefly summarize the work completed in the past calendar year regarding nuclear-specific FeCrAl compositions as well as a brand new section on fatigue after finding additional past literature. Finally, small technical and grammatical updates were included in previous sections to provide a more robust and polished handbook. The primary technical difference between the previous version and the new revision is the

inclusion of recent results from ATR, Halden, MITR, and Hatch 1 on integral tests, a key component missing in the irradiated FeCrAl database. (Y. Yamamoto)

- **[ORNL]** A manuscript is in process on yttrium effects on the grain stability of ferritic alloys (Gen. II FeCrAl alloys and two additional model alloys) at high temperatures. The elemental yttrium segregation on grain boundary as well as yttrium rich particles played an important role of refining and stabilizing the grain size of bcc α-Fe matrix, which could be beneficial for improvement of room-temperature deformability, and therefore, the processability of thin-wall seamless tube production. (Z. Sun, Y. Yamamoto)
- **[ORNL]** Evaluation of minor alloying effects on microstructure evolution has been initiated by using C26M (Fe-12Cr-6Al-2Mo-0.2Si-0.03Y, wt.%) base alloys. Grain refinement was observed by using a certain amount of carbon addition, which could be another potential to control the grain refinement to improve the deformability of ATF FeCrAl alloys. (Y. Yamamoto)
- **[ORNL]** The Level 2 milestone report M2NT-18OR020202101 titled, "Handbook of LWR SiC/SiC Cladding Properties - Revision 1," has been completed. Properties of SiC composites for better multi-physics modeling of ATF SiC cladding were summarized. The report presents various properties, including mechanical and thermal properties, chemical stability under normal and off-normal operation conditions, hermeticity, and irradiation resistance. The report was submitted on August 2, 2018. (T.Koyanagi, Y.Katoh)

LWR Irradiation Testing & PIE Techniques

- **[INL]** Cycle 164B-1 was completed. The Data Package revision and basket loading calculations were completed to support reconfiguration activities at ATR. Reconfiguration of the ATF-1 experiments was successfully completed. (D. Dempsey)
- **[INL]** ATF-2 irradiation was completed during Advanced Test Reactor Cycle 164A reaching 54 effective full power days. (G. Hoggard)
- **[INL]** Data from PIE is being compiled into the end of the year milestone report and manuscripts for publication in peer reviewed journals. A draft article is currently under review at Framatome. (J. Harp)

LWR Fuel Safety Testing

- **[INL]** Assembly of first and second capsules for TREAT irradiation was completed and the first capsule was shipped to TREAT for assembly into the test vehicle. The second capsule will be shipped to TREAT on September 5. At this time all experiment hardware has been delivered to TREAT to support the first fueled TREAT experiment irradiation since the TREAT restart. (D. Dempsey)
- **[INL]** The Functional & Operational Requirements (F&OR) for MARCH-SERTTA and Super-SERTTA are out for review and approval. Work continued on the Super-SERTTA conceptual design and the MARCH-SERTTA preliminary design. (J. Schulthess)
- **[ORNL]** A publication titled, "Surface wettability and pool boiling Critical Heat Flux of Accident Tolerant Fuel cladding-FeCrAl alloys," was published in Nuclear Engineering and Design [Ali et al., 338 (2018) 218-231]. The manuscript analyzes the impact of surface roughness and oxidation on wettability and critical heat flux. Experimental data was then compared to these critical heat flux values and departure from nucleate boiling radios as calculated using the COBRA-TF subchannel code to simulate behavior in a PWR. The results found that oxidized FeCrAl performed better than Zirc-4 throughout the assembly, suggesting that FeCrAl may be able to better withstand hypothesized

accident conditions without leading to a boiling crisis scenario. (A. Ali, J. Gordon, N. Brown, K. Terrani, C. Jensen, Y. Lee, E. Blandford)

- **[INL]** The Level 2 Milestone titled, "Complete design and build experiment support equipment to support instrumentation and controls for each experiment," was completed on August 30, 2018. (T. Pavey)
- **[INL]** The instrument hardware including complete custom INL-built fiber assemblies has been delivered and is now being assembled to support the ATF-SETH tests. (T. Pavey)
- **[INL]** The high temperature test station for LVDT (elongation sensor) characterization has been finalized and has been automated to expedite sensor evaluations. (T. Pavey)
- **[INL]** MAMMOTH multi-physics calculations have been completed for the ATF-3-1 transient prescriptions for both the 1.5% and 2.6% Δk/k transients. Transient power results are in good agreement, although MAMMOTH calculates a slightly shorter period than was measured, with a peak power slightly higher than measured, occurring at approximately 0.2s in the 1.5% case and about 0.1s in the 2.6% case. The reason for this discrepancy has not yet been identified, but may be due to the value of the mean neutron lifetime used. However, calculations for the power coupling factors for the five sample wires were in extremely good agreement with measurement, with a relative error of 0.44 +/- 2.6% for the 1.5% transient (0.11 +/- 4.1% for MCNP simulations), and 0.78 +/- 2.3% for the 2.6% transient (0.8 +/- 3.7% for MCNP). Both show very little bias in the calculations, but MAMMOTH calculations show less uncertainty relative to measurements. Current efforts are examining SPND data from in-core measurements to determine if a more accurate period is measured within the center of the core. (T. Pavey)
- **[INL]** The MARCH-SETH experiment is currently being evaluated with a 5x5 core configuration to determine the most appropriate cross section treatment for this configuration. Generation of super-homogenization (SPH) factors is being found difficult to converge; there are a significant number of streaming regions in this configuration. At present Tensor Diffusion Coefficients (TDCs) are being computed for various regions in the core, vehicle and inside the canister, since it is a dry experiment. TDCs allow introduction of directionally dependent diffusion coefficients to account for directional streaming effects. (T. Pavey)

LWR Computational Analysis & Fuel Modeling

- **[BNL]** Advanced LWR Fuel Concept Analysis, NT-18BN02020501, an effort has been initiated to set up an uncertainty analysis framework to identify and quantify all potentially important parameters that impact the TRACE systems analysis code predicted figures of merit, such as the peak cladding temperature (PCT) and the amount of hydrogen generation. The approach is to use the TRCAE-DAKOTA interface in SNAP (a graphical user interface to perform TRACE runs) to create uncertainty job streams, executing TRACE runs and generating DAKOTA reports (including, e.g. PCT distribution and importance ranking of parameters). Progress has been made in testing the TRACE-DAKOTA interface in SNAP (a graphical user interface for TRACE) to perform an uncertainty analysis to evaluate the importance ranking of parameters, such as, fuel and cladding thermal conductivity, hot rod peaking factor, etc. (L-Y. Cheng)
- **[BNL]** Several options for coating fuel pellets to mitigate the fuel/coolant interactions for water-reactive high-density fuel phases, such as U3Si2, and UN have been proposed by LANL. Initial modelling of these options with the TRITON neutronic lattice physics code to provide an initial estimate of the impacts on reactor performance and safety characteristics is underway. Two options are being evaluated: 1) coating of the fuel pellet; and 2) coating of individual fuel particles. Analyses have been completed for 20 μm coatings of Zr-metal, ZrB2, Y2SiO5, Cr-10Al, and AlN on UN and on U3Si2 (except for AlN). The analyses all assumed the standard Westinghouse 17x17 assembly

geometry and fuel pellet OR and Zircaloy cladding IR/OR; therefore, the gap was reduced by the thickness of the coating. The nitrogen for all cases, and the boron for zirc-diboride, were "natural". The burnups for the different coatings are all essentially the same, and only slightly lower than for the "reference" UO2-Zr case. The reactivity and control coefficients (fuel and moderator temperature coefficients, and soluble boron and control rod worths) are effectively the same for all the coatings for the 20 μm thickness. Calculations for 40 μm coatings and "particle coatings" are underway. (M. Todosow, A. Cuadra)

- **[ORNL]** The QUENCH-19 test of FeCrAl(Y) was successfully performed on August 29 at KIT in Germany. The QUENCH facility provides the capability to perform an experimental simulation of severe accidents as a function of temperature and coolant flow / condition while measuring hydrogen generation. This allows for determination of the hydrogen source term, temperatures or thresholds where core geometry is lost, or how reflooding affects behavior. The QUENCH-19 test was performed to compare a FeCrAl(Y) alloy, (B136Y3) to ZIRLO under similar flow and power conditions of a beyond design basis LOCA. Preliminary analysis of the test results show that hydrogen production in FeCrAl was nearly an order of magnitude lower than ZIRLO and did not experience rapid temperature escalation as would occur due to oxidation of zirconium. Data analysis and modeling of the QUENCH-19 data will continue into FY19 to better understand the behavior of FeCrAl as an ATF cladding during beyond design basis transients. (A.Nelson, K.Robb, K.Terrani)

Industry FOA

- **[INL]** PLN-5612, "U3Si2 Fuel Pellet Fabrication Plan," was issued. PLN-5636, "CHNO Analysis of U3Si2," was completed. PLN-5637, "Test Control Plan for Determining Enrichment, U, Si, and Impurity Content of U3Si2 Pellet Fuel Analytical Chemistry Methods," was completed. PLN-5638, "X-Ray Diffraction Phase Identification of Uranium Silicide (U3Si2)," was completed. Analytical Laboratory analysis of the depleted uranium dry run pellets was completed. Analytical Laboratory analysis of the enriched uranium "Batch 0" pellets was completed. The laboratory analysis for phase purity of the enriched uranium "Batch 0" pellets was completed. Laboratory analysis for grain size of the enriched uranium "Batch 0" pellets was completed. (S. Martinson)
- **[ORNL]** The Level 3 milestone M3NT-18OR020206061 titled, "Steam Oxidation, Burst and Critical Heat Flux Testing of FeCrAl Cladding in the Severe Accident Test Station," due on August 3, 2018, was successfully completed. The corresponding report describes the use of FeCrAl (C26M) tubing to conduct additional steam oxidation testing as well as additional burst testing. This is the same C26M material that was loaded into Plant Hatch in February 2018 and its oxidation resistance and burst resistance are superior to the 1st generation FeCrAl material. We also are exploring ways to study critical heat flux (CHF) conditions in the Severe Accident Test Station (SATS). We have successfully modified the software and hardware to conduct this type of experiment and showed a comparison between C26M and a Zr-based tube. As expected, the C26M tube showed less deformation and less oxidation that the Zr alloy tube during cycling in steam to 650°C with a 5 MPa internal pressure. Additional CHF experiments will be conducted when more Zr alloy tubing is obtained for comparison to C26M. In addition, this report will be circulated with industrial partners to allow comment on the parameters chosen for the proposed CHF experiments. Additional oxidation and burst testing also is in progress to provide statistical information on these results for modeling various accident conditions. (B.Pint)

ADVANCED REACTOR FUELS

AR Fuels

- **[INL]** The Level 3 milestone titled, "Report on Americium Volatility," was met on time. Most of the metallic transmutation fuel concepts include americium as a fuel component, however, concerns have persisted as to whether the volatile americium can be retained during the casting process. A series of experiments were conducted in which U-7Pu-1.6Am alloy was produced, and heated to 1400° C, and held for 15 minutes. The heating tool was placed under the following atmospheric pressures; 1) flowing argon 2) 400 torr argon over pressure 3) 200 torr argon over pressure and 4) active vacuum. After each heating cycle, the mass of individual components was measured and tracked from runs to run. In addition to the mass, radiation dose rates were also measured from various components after each cycle. Table 1 provides a summary of the mass balance results, while Figure 2 shows a graphical representation of the dose rates from run to run. The data shows that americium can be retained with very modest overpressures of argon. (R. Fielding)

  Table 1. Summary of mass changed of the alloy and crucible assemble from run to run.

	Pre Run 1	***Post Run 1***	***Pre Run 2***	***Post Run 2***	***Pre Run 3***	***Post Run 3***	***Pre Run 4***	***Post Run 4***
Total charge/ingot (g)	*77.778*	*77.715*	*77.143*	*77.088*	*76.820*	*76.750*	*76.472*	*75.625*
Δ *ingot (g)*	*0.063*		*0.055*		*0.07*		*0.847*	
Y_2O_3 crucible (g)	*41.317*	*41.361*	*41.361*	*41.405*	*41.405*	*41.473*	*41.473*	*41.364*
Δ *Y_2O_3 crucible (g)*	*0.044*		*0.044*		*0.068*		*-0.109*	
Graphite crucible (g)	*53.147*	*53.100*	*53.100*	*53.070*	*53.070*	*53.041*	*53.041*	*53.295*
Δ *graphite crucible (g)*	*-0.047*		*-0.03*		*-0.029*		*0.254*	
Graphite lid (g)	*8.022*	*8.021*	*8.021*	*8.019*	*8.019*	*8.017*	*8.017*	*8.671*
Δ *graphite lid (g)*	*-0.001*		*-0.002*		*-0.002*		*0.654*	

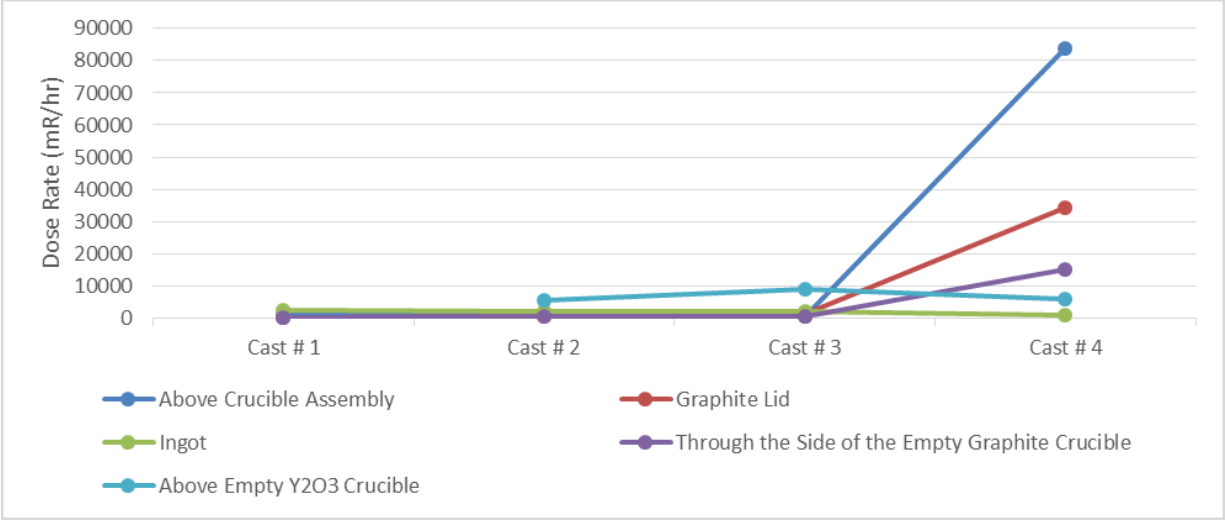

Figure 2. Radiation dose rate changes from heating cycle to heating cycle.

- **[INL]** The Level 2 milestone titled, "Demonstrate U-Zr Annular fuel fabrication through extrusion," was met on time. Annular fuel has been proposed as an advanced fuel concept which may provide significant improvements on burnup capability and used fuel disposition. However, producing annular fuel through standard casting processes is not feasible. Extrusion provides a feasible path to produce this fuel form. A U-10Zr billet was cast and machined, then hot extruded. The billet was heated to 800°C, with an outside diameter of approximately 8.6 mm, while the internal mandrel was 6 mm. Although optimization is required, by meeting this milestone it has been shown that U-10Zr fuel can be extruded into an annular form using largely standard processing equipment and techniques. Figure 3 below shows the final extruded product. (R. Fielding)

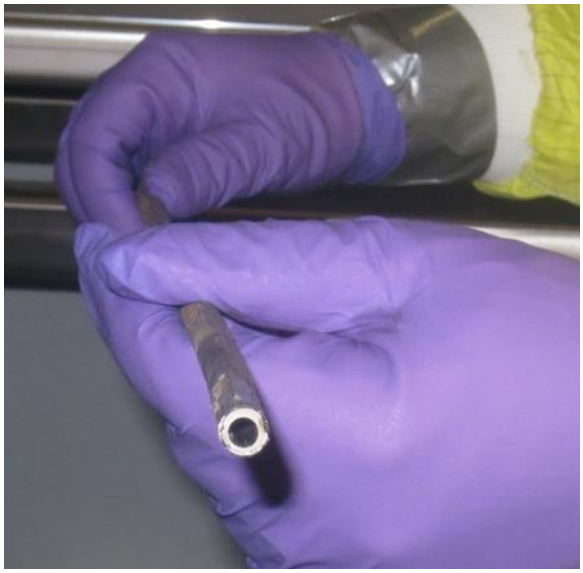

Figure 3. Extruded annular U-10Zr.

- **[INL]** The next irradiation test that is currently planned is the FAST test, which utilizes sub-sized specimens in order to obtain higher burnup values in shorter times. One of the difficulties expected in fabrication of this test will be the casting of the fuel with a diameter of approximately 2.1 or 1.4 mm. AFC fuel has traditionally been cast using the arc melting technique. Using this technique, generally

the only driving force for casting is gravity. Because of the small diameter of the test samples, gravity alone will not be sufficient because of the high surface tension of the molten materials. As previously reported, to overcome the surface tension a small vacuum assisted casting apparatus was designed and fabricated and was used to fabricate 2.1 mm diameter fuels. This work has continued by casting 1.4 mm diameter slugs of both U-10Zr and uranium. It was discovered that as the casting trials continued the copper hearth increased in temperature, which led to the casting of higher quality pins. Figure 4 shows a typical example of a cast pin. (R. Fielding)

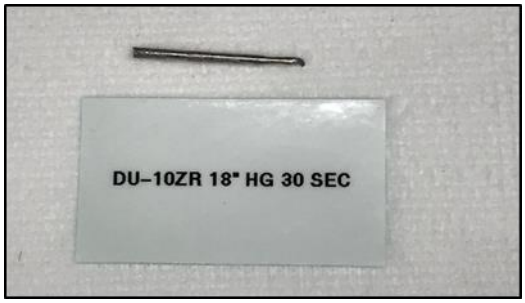

Figure 4. Example of a cast pin.

- **[INL]** The Level 2 milestone report titled, "Issue Update of Metallic Fuels Handbook," was completed on August 27, 2018. (C. Papesch)

AR Core Materials

- **[PNNL]** A manuscript titled, "The Application of the OPTICS Algorithm to Cluster Analysis in Atom Probe Tomography Data," written by Jing Wang has been accepted for publication in Microscopy and Microanalysis. This manuscript presents a new, simpler and potentially more accurate algorithm created by Jing Wang to identify precipitates in atom probe tomography data sets. The algorithm utilizes an open source subroutine called OPTICS. PNNL is now routinely using this algorithm for precipitate identification in our APT data sets. (M. Toloczko)
- **[ORNL]** Residual stresses were calculated from residual strains measured at the HB-2B Neutron Residual Stress Facility beam line at HFIR in 2017 for 4 (R1, R2, R3 and R4) plates of 14YWT (SM13 heat) that were hot rolled to thicknesses of 10, 5, 2.2 and 1 mm (up to 95% reduction in thickness). The residual stress data was plotted in 2-D contour maps using Origin 2018 to show the spatial distribution and magnitude of the residual stresses as a function of rolling deformation. The results showed a slow increase in residual stress in the extrusion direction (ED) and rolling direction (RD) after rolling deformations of 50% (R1), 76% (R2) and 89% (R3). After 95% (R4) rolling deformation, the residual stresses in these two orientations increased abruptly up to levels of 600-800 MPa. The residual stresses for the normal direction were similar for all 4 rolled plates and were generally <200 MPa. These results highlight the importance of measuring residual stresses to help mitigate welding problems caused by friction stir welding and implement pre- or post- welding heat treatments to lower the internal stresses. (D. Hoelzer)
- **[ORNL]** A sample of the 1.0 mm thick 14YWT plate containing the friction stir weld (FSW) butt joint was prepared by metallographic procedures. The sample broke in half along the butt joint during cutting indicating residual stresses in the butt joint were high. The microstructure of the butt joint and surrounding thin plate of 14YWT was examined by SEM and electron backscattered diffraction (EBSD). Strong <110> texture and highly elongated grains were observed in the 1.0 mm thick plate of 14YWT that changed to equiaxed, slightly coarsened, grains with random texture in the butt joint. A non-uniform distribution of pores was present in both the advancing and retreating sides in the butt joint. The SEM and EBSD results highlight the effects of the FSW conditions on altering the

microstructure of 14YWT from highly textured rolling condition to random texture in the butt joint. (D. Hoelzer)

- **[PNNL]** As part of the program to advance the technology associated with fabricating tubing from difficult-to-fabricate materials, the PNNL rolling mill is being modified so that it can perform pilgering of tubes. This will establish a unique R&D capability within the DOE complex. In order to modify the rolling mill so that it can perform pilgering, a set of rollers unique to the pilgering process and the rolling mill are required. These rollers were machined by Precision Products, have arrived at PNNL, and are shown in Figure 5. The plan is now to install the rollers on the rolling mill and program the electronic control system with the correct rotation and feed rates for pilgering. It is planned to perform the initial pilgering runs in September. (R. Omberg)

Figure 5. Rollers to perform pilgering.

- **[PNNL]** Fracture toughness testing for the two HT-9 steels with low and high nitrogen after single and double step tempering treatments was completed. More than 120 miniature fracture specimens (4 mm x 2.5 mm x 13 mm) with various quenched and tempered martensitic structures were produced by combining a rapid water quenching (WQ) and 9 nontraditional tempering treatments and were tested at 22(RT), 200, 300, 400, 500 and 600°C. The fracture toughness at RT is generally quite high (i.e., > ~200 MPa√m) except for the samples before tempering or after low temperature (< 500°C) tempering and the temperature dependence of fracture toughness above RT is strongly dependent on the degree of tempering. It is notable that the HT-9 heat-3 samples after WQ + 500°C tempering and WQ + 600°C tempering show ~20% higher fracture toughness at 600°C (250 and 230 MPa√m, respectively) when compared to those of typically treated HT-9 steels. Overall, the mechanical properties of HT-9 steels varied widely with their processing routes, particularly with the degree of tempering. The best processing route, which consists of a rapid quenching and a limited tempering (WQ-500°C) yielded excellent strength (> 0.9 GPa up to 500°C) with improved high temperature fracture toughness. Further characterization for the HT-9 alloys after such optimized processing will be pursued. (T.S. Byun)

AR Irradiation Testing & PIE Techniques

- **[INL]** Irradiation cycle 164A-1 was completed and the cycle analysis for cycle 164B-1 was started. A new process for cycle analysis is being implemented in order to support shorter outage durations at ATR. (D. Dempsey)
- **[INL]** Data from PIE of AFC-3C, AFC-3D, AFC-4A and other irradiations is being compiled into the end of the year milestone report and manuscripts for publication in peer reviewed journals. (J. Harp)

CAPABILITY DEVELOPMENT

CX Fuels

- **[INL]** The Level 2 milestone titled, "Closeout Phase II Qualification of the Thermal Conductivity Microscope for IMCL," – NT18IN02030101 was completed on August 28, 2018. (D. Hurley)

For more information on Fuels contact Steven Hayes (208) 526-7255.

Material Recovery and Waste Forms Development

PROCESS CHEMISTRY AND INTEGRATION

- **[INL]** All experimental studies for N-methylpyrazine-diethylenetriamine-N,N',N",N"-tetraacetic acid, DTTA-PzM, have been completed in preparation for the submission of the journal article. This aminopolycarboxylate reagent follows the previously reported structural modification utilizing the N-methylpyridine substitution of diethylenetriamine moiety. (Grimes, T.S. et al., Inorg. Chem., 2018, 57, 1373) A transition to a more acidic pyrazine N-heterocycle maintains the An3+/Ln3+ differentiation afforded by the N-methylpyridine-substituted reagent in aqueous mixtures containing roughly 10 times the concentration of hydrogen ion. (P. Zalupski)
- **[INL]** Di-2-ethylhexylbutyramide (DEHBA) has been proposed as part of a hydro-reprocessing solvent extraction system for the co-extraction of uranium and plutonium from spent nuclear fuel, owing to its selectivity for hexavalent uranium and tetravalent plutonium. However, there is a critical lack of quantitative understanding regarding the impact of chemical environment on the radiation chemistry of DEHBA, and how this would affect process performance. A systematic investigation has been performed into the radiolytic degradation of DEHBA in a range of n-dodecane solvent system formulations, where we subject DEHBA to gamma irradiation, measure both ligand integrity and degradation product formation, and investigate solvent system performance through uranium and plutonium extraction and strip distribution ratios. The rate of DEHBA degradation was found to be slow (an average of 0.33 μM J−1) and dependent upon the oxidizing conditions of the investigated solvent systems (organic only, or in contact with either 0.1 or 4.0 mol·L−1 aqueous nitric acid). Two major degradation products were identified in the organic phase, bis-2-ethylhexylamine (b2EHA) and mono-ethylhexylbutyramide (MEHBA), but these could not account for the total loss of DEHBA, indicating extensive secondary radiolysis. No significant degradation products were identified in the aqueous phase, despite a very rigorous analytical protocol. Solvent extraction studies showed: (i) uranium extraction and stripping generally decreased with increasing absorbed dose; (ii) plutonium extraction was enhanced through the formation of a secondary DEHBA degradation product, inhibited by nitric acid; and (iii) enhanced plutonium retention in the organic phase, indicating the formation of a second plutonium complexing species. This draft manuscript has been prepared in fulfillment of Milestone M3NT-18IN030102031. (G. Horne)
- **[ORNL]** The evaluation of larger cation exchanged Cs-LTA membranes was initiated. It is thought that the selectivity and separation factor of HTO/H2O could be substantially higher for ion-exchanged LTA zeolite membranes with larger cations. As reported in the last monthly report, RbA zeolite (2.5 Å < dp < 2.9 Å) and CsA (≈ 2.5 Å) have smaller effective opening diameter (dp) than KA zeolite (≈ 3.0 Å) or NaA zeolite (≈ 4 Å).

  Table 1 summarizes the results for K-LTA and Cs-LTA zeolite membranes. As can be seen, the separation factor of HTO/H2O with Cs-LTA is substantially higher than the highest calculated separation factor with K-LTA zeolite membranes. This is very encouraging, and we plan to perform additional experiments in September to confirm these results. Based on the techno-economic analysis completed in FY17, it was shown that a high separation factor will have a major impact on the number of stages required to achieve the desired composite separation factor of 100. We believe that further improvements are possible and plan to investigate larger cations such as rubidium, and membrane optimization to increase permeance and separation factor. (B. Jubin)

Table 1. Permeance and separation factor of tritiated water results Cs-LTA on CoorsTek alumina disk support

Expt.	Membrane	pH	Radioactivity (mCi/mL)			Permeance (GPU)		Separation factor (α)
			Feed	Retentate	Permeate	HTO	H_2O	
1	**K-LTA**	7	0.8919	0.9189	0.8108	3906	3586	1.10
2	**Cs-LTA**	7	0.7567	0.7027	0.4054	360	561	1.87
3	**Cs-LTA**	7	0.5405	0.5135	0.2567	266	467	2.11

- **[ORNL]** The previously prepared grout waste forms containing surrogate UNF were leached using the ANSI/ANS 16.1 methodology and the leachates analyzed for U and Cs, Sr, La and Ce using inductively coupled plasma mass spectrometry. The analytical results are being tabulated, analyzed, and will be reported in the final September milestone report. (B. Jubin)
- **[PNNL]** The M4 milestone (M4NT-18PN030102072), QRL4, "Development & Application of Optical Spectroscopy for Monitoring within Microfluidic Devices," with a due date of 8/31/2018 was completed during the reporting period by submission of a peer-reviewed manuscript to the American Chemical Society journal, Analytical Chemistry. The title of the paper is "On-line monitoring of solutions within microfluidic chips: simultaneous Raman and UV-vis absorption spectroscopies." This manuscript describes the use of simultaneously applying micro-UV-vis and micro-Raman spectroscopies adapted to function on the microscale to analyze both the Nd3+ (UV-vis active) and HNO3 (Raman active) concentrations, in-situ, within a microfluidic device (MFD), on the same flowing sample stream. These complimentary spectral techniques when processed through multivariate PLS (Partial Least Squares) models gave an accurate picture of the widely varying solution concentrations as a function of time for each solution component. Solution matrix effects can drastically alter analyte signatures as measured by both UV-vis absorbance and Raman spectroscopy. PLS methods successfully modeled these spectral changes and accurately measured concentrations of components of interest within the microfluidic chip. This work is the product of a collaboration between Pacific Northwest National Laboratory, the College of Idaho, and Spectra Solutions, Inc. The authors on this submission are Gilbert Nelson (College of Idaho), Amanda Lines, Job Bello (Spectra Solutions Inc.), and Samuel Bryan. (S. Bryan)

SIGMA TEAM FOR ADVANCED ACTINIDE RECYCLE

- **[INL]** A conceptual group hexavalent actinide co-crystallization separation process has been developed using experimental solubility data for actinides and key fission products. This flowsheet considers the basic reprocessing unit operations required for head-end and crystallization separation processes for group actinide recovery from irradiated commercial light water reactor fuel.

  Np, Pu, and Am are oxidized to a hexavalent state in a used nuclear fuel dissolver product solution using excess sodium bismuthate. Cooling from 58°C to 20°C at a controlled rate promotes crystal growth of hexavalent U, Np, Pu, and Am in the primary crystallizer. A second crystallizer unit provides further decontamination from fission products that are either co-crystallized or entrained on the crystals after filtration of the mother liquor from primary crystallization. Recycle loops are implemented that maximize recovery of both uranium and transuranic elements. Using this conceptual two-stage co-crystallization flowsheet concept, the recovery for U, Np, Pu, and Am was calculated to be 64%. Exceptional decontamination from key fission products Cs+, Sr2+, Nd3+, and Zr4+ was achieved with a calculated U-TRU crystalline phase purity of 99.999%.

- Preliminary calculations suggest that a reprocessing flowsheet utilizing group co-crystallization of hexavalent actinides shows promise for a simple single-step group actinide separation process that reduces the volume of liquid high level waste generated. Recovery must be improved using mother liquor recycle loops for the process to be viable. Challenges and limitations of the concept flowsheet are addressed to identify focus areas for future development in actinide crystallization flowsheets. (K. Lyon)

WASTE FORM DEVELOPMENT AND PERFORMANCE

Electrochemical Waste Forms

- **[ANL]** Technical reports detailing the development and corrosion behavior of representative alloy waste forms RAW-2 and RAW-4 and three variations of RAW-6 are being finalized. The experimental protocol and analysis methods used were developed to support and parameterize the degradation model following the approach outlined in the roadmap report FCRD-2013-000226. The RAW-6 alloy made with added U and Tc is a nearly optimized formulation for waste forms made with 316- and HT9-type cladding. The formulation, test methods, and models that are used take the beneficial effects of passivating elements (particularly Mo and Cr) into account. The noble metal waste constituents (primarily Ru and Pd) are observed to have significant effects on the corrosion behavior due to localized H2 generation. For example, Figure 6 compares the responses of RAW-6 materials made with Re as a surrogate for Tc, with U, and with both U and Tc in electrochemical tests conducted in 0.01 M NaCl solutions adjusted to pH 3 or pH 8. The potentiodynamic scans in Figure 6a and currents in Figure 6b show the stabilization of RAW-6(U) relative to RAW-6(Re) provided by the addition of extra Mo and the further stabilization of RAW-6(UTc) by the addition of Tc. The extra Mo in RAW-6(U) and RAW-6(UTc) resists pitting and supports formation of a NiMoO4 passive layer that is effective at applied potentials above about 400 mV. The mass corrosion rate is proportional to the current density. Tests show the corrosion rate increases slowly with the potential, but is mostly insensitive to pH within the stability fields of the passivating oxides (and the conditions expected in a disposal system). (W. Ebert)

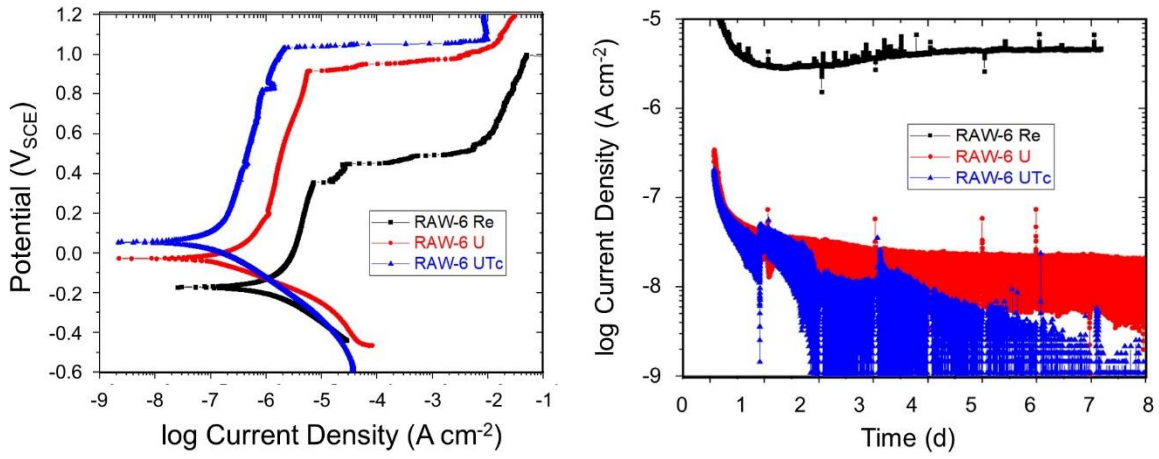

(a) (b)

Figure 6. Results of tests with RAW-6 alloys with added Re, U, and both U and Tc: (a) potentiodynamic scans in 0.01 M NaCl adjusted to pH 8 and (b) current densities measured in potentiostatic tests at 300 mV$_{SCE}$ in 0.01 M NaCl adjusted to pH 3.

Ceramic Waste Forms

- **[SRNL]** The feed materials for glass-ceramic pour have been ordered. The CRADA with ANSTO is in the process of being extended to FY20. (J. Amoroso, P. Smith)

Glass Ceramics Waste Forms

- **[LANL]** A series of hollandite type materials, powellite type materials, and oxyapatite materials which are major crystalline phases in our multiphase ceramic and glass ceramic waste forms, have been irradiated with alpha (He) and Kr ions (separately) at LANL, with dual ion beams (He and Kr ions simultaneously) at the IVEM facility at ANL. Ion irradiation is used to simulate alpha decay in nuclear waste materials. Further characterizations will focus on irradiation damage induced swelling, microcrack formation, and structural evolutions in these materials. (M. Tang)
- **[PNNL]** The paper titled, "Synthesis and characterization of oxyapatite [Ca2Nd8(SiO4)6O2] and mixed-alkaline-earth powellite [(Ca,Sr,Ba)MoO4] for a glass-ceramic waste form," was accepted by the Journal of Nuclear Materials. This article documents synthesis of two key crystalline phases found in the glass-ceramic waste form. They are being studied to determine their corrosion properties individually to further understand elemental releases from the complex glass ceramic. (J. Crum)

Zirconium Recycle

- **[ORNL]** Mass spectrometer results on the effluent fractions from the first ZrCl4 purification test were received during August. Overall, the analytical results show that the purification factor for 94Nb was 8, similar to initial results for non-radioactive tests obtained at UTK, with a purified Zr recovery of 60%. The PF for 125Sb was only 4; and subsequent HSC calculation indicates that the condensed ZrCl4 should be held at 200-250 C under a H2 atmosphere. In the first purification test with radioactive material, we were unable to use pure H2 in the glove box because of safety concerns that it might be diluted into the explosive region. Previous cold tests indicated that using 4%H2/N2 was not effective. However, UTK researchers are now finding that 4% H2/N2 can be partially effective by increasing the reaction time and raising the temperature to 290 C. This method will be used in the next hot purification test. Also, without using H2, no purification from iron was achieved. The use of ZrH2 has been successful as a combination as a reducing agent for both NbOCl3 and FeCl3 in previous cold tests and will be used at low concentration in future purification tests to avoid fire hazard safety concerns. (B. Jubin)

Advanced Waste Form Characterization

- **[ANL]** The manuscript titled, "Parameterizing a Borosilicate Waste Glass Degradation Model," was submitted to npj Materials Degradation for publication (milestone M3NT-18AN030105082). The paper describes recent tests to evaluate the dependencies of the rate terms used in the ANL Stage 3 glass degradation model on the solution pH, Al and Si concentrations based on novel modified PCTs in which those variables were modified when the tests were initiated. The method was applied in tests with AFCI and LRM glass and found to successfully distinguish between the influence of the solution composition on the dissolution rates and the influence of the dissolution rates on the solution compositions. For example, Figure 7a shows the residual rates are independent of the Si concentrations and the pH decreased before Stage 3 was triggered in tests with AFCI glass and Figure 7b shows the Stage 3 rates are correlated with both the pH and the Si concentration. The correlation with the Si concentration is a result of glass dissolution but the correlation with pH probably shows its effect on the rate. The low Al concentrations neither affect nor are affected by the Stage 3 rate. It is planned to apply the method to other glasses in FY19 to verify the rate dependencies and to reassess results compiled in ALTGLASS database to derive model coefficients for the Stage 3 model. A separate report that fully documents the test results is being finalized. (W. Ebert)

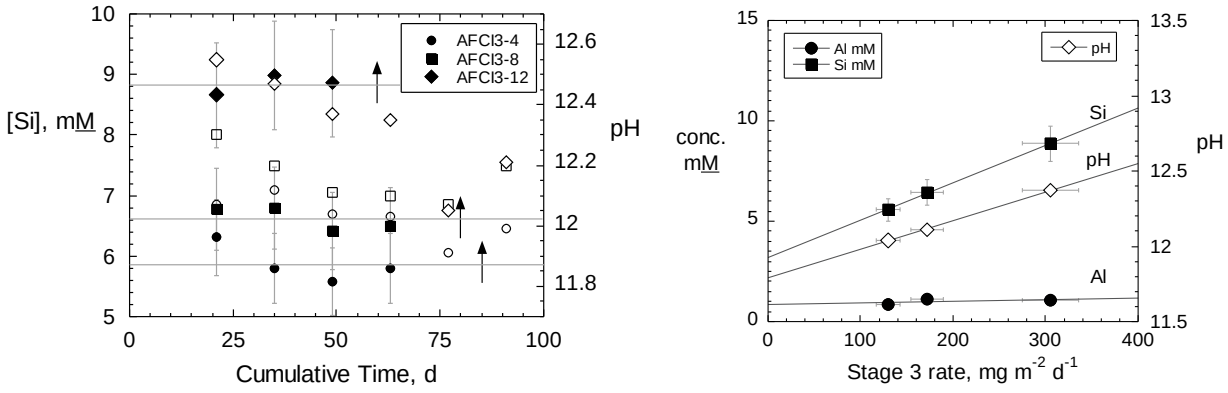

(a) (b)

Figure 7. Results of modified PCT with AFCI glass at 90 °C showing (a) pH and Si concentrations measured before Stage 3 and (b) correlations of Stage 3 rate with pH, Al and Si concentrations.

- **[PNNL]** The most potentially impactful aspect of glass corrosion behavior is the resumption of a relatively high dissolution rate coincident with the formation of zeolitic secondary phases that has been seen in tests with many surrogate waste glasses. Predicting if and when this behavior, termed Stage III behavior, will occur under disposal conditions and the potential impact remains the major challenge in assessing the long-term performance of borosilicate glass waste forms. This month, researchers from PNNL and ANL produced a joint report that details the ongoing work to inform and develop a glass degradation model that can be used to demonstrate the safe disposal of high-level radioactive waste glasses produced at DOE facilities. Experimental efforts are, in general, being targeted to elucidate mechanisms, provide actionable information about Stage III behavior, or both. Because the solution pH and concentrations of glass constituents evolve simultaneously as the glass dissolves, test methods have been developed and are being standardized to distinguish between the effects of individual variables. Including the contributions from the DOE Office of Environmental Management, other experimental and modeling efforts are investigating mechanisms affecting the other rate-behavior stages to provide functional rate models in each case with solid scientific support. This includes multiple investigations into the mechanisms that drive the decrease in the Stage II rate; e.g., the evolution of alteration layers, transport processes through porous layers, ion exchange processes, and how the Ostwald ripening of secondary phases affects the long-term glass dissolution kinetics. The experimental work and continued utilization of results available in the ALTGLASS database feeds efforts to develop and parameterize models of Stage III behavior, including both operationally-focused empirical bounding models and more detailed mechanistic models. The work is continuing in partnership with the performance modeling team in the Used Fuel Disposition Campaign to ensure that the Stage III models fit seamlessly into the more general repository models. (J. Ryan)

DOMESTIC ELECTROCHEMICAL PROCESSING

- **[ANL]** Work plans are being developed for pyroprocessing R&D activities in electroreduction of oxide fuel and waste form development under the auspices of the Civil Nuclear Energy Working Group project arrangement between Japan and the United States. Work at ANL includes evaluation of the behavior of Zr alloys and zirconates formed during the oxide reduction process as a function of processing conditions and comparative assessments of salt treatment methods and waste forms. ANL will also provide expertise supporting metal waste form production at INL based on recent formulation and testing of steel-based alloy waste forms. (W. Ebert)

SIGMA TEAM FOR OFF-GAS

- **[INL]** A long-term deep-bed adsorption test was started for capturing organic iodide species in simulated vessel off-gas (VOG) from aqueous used fuel reprocessing. The simulated VOG is air with a target 1 ppm concentration of iodobutane (C4H9I) as a surrogate for a range of possible organic iodides that could be present in VOG. This iodobutane concentration represents the high range of expected organic iodide concentrations in VOG. Preliminary results in Figure 8 and Figure 9 show that the adsorption of iodine onto the sorbent, silver Aerogel, follows the expected mass transfer zone (MTZ) concept, where most of the iodine is adsorbed near the front of the sorbent bed, in the MTZ. No measureable adsorbed iodine was detected in the sorbent beyond 4.5 inches deep after operation for over 500 hours. This test is planned to continue until the MTZ progresses into the bed so that the front end of the sorbent bed approaches its practical saturation concentration and maximum silver utilization, and so that the depth of the MTZ can be determined. Thus far in the test, these results are consistent with results from tests with simulated dissolver offgas, although with lower inlet organic iodide concentrations, the test duration will need to be longer. (J. Law)

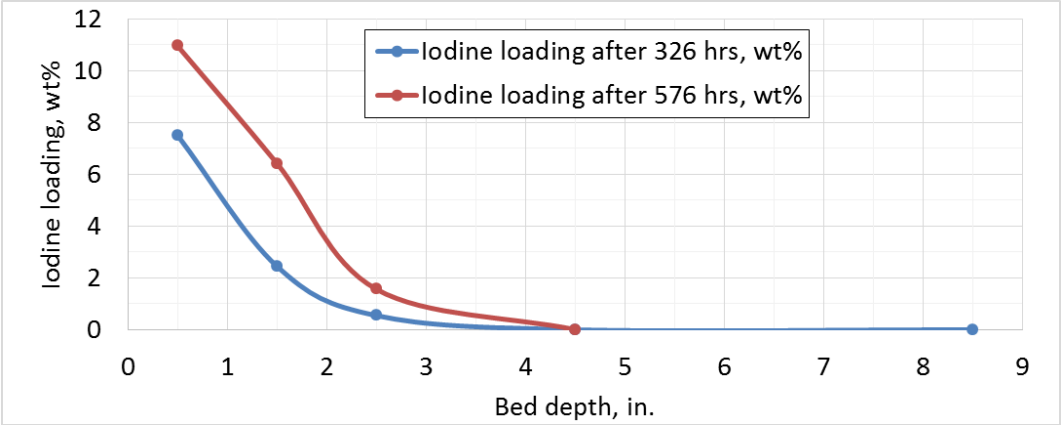

Figure 8. Iodine loading on Ag Aerogel sorbent during simulated VOG testing with a target 1 ppm iodobutane concentration in the inlet simulated VOG.

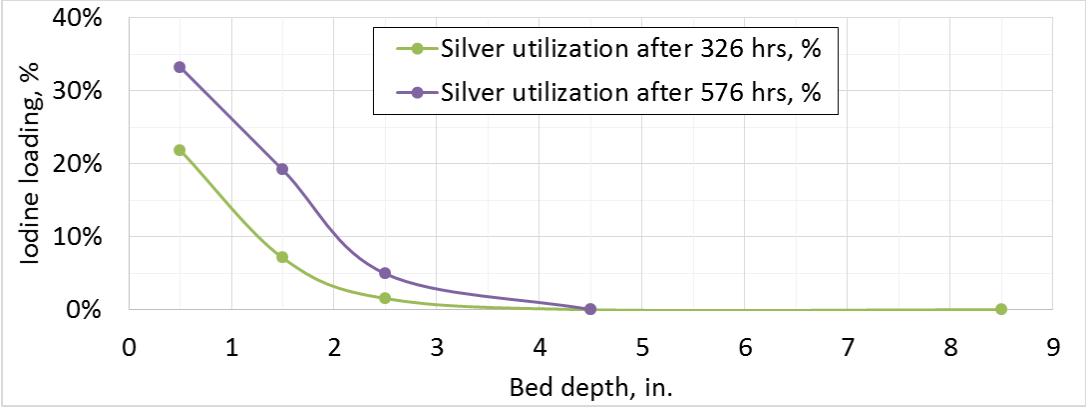

Figure 9. Iodine loading on Ag Aerogel sorbent during simulated VOG testing with a target 1 ppm iodobutane concentration in the inlet simulated VOG.

- **[INL]** A report titled "HZ-PAN and AgZ-PAN Desorption Characterization," was completed, meeting the Level 3 milestone INL- M3NT-18IN030107011. The report documents a series of tests focused on stepwise thermal desorption to characterize the bulk gases removed from AgZ-PAN and

HZ-PAN and relative separation of Kr and Xe from each other and from the bulk air. The result was 99-100% separation of Xe from Kr, and 77-83% separation of Kr from air while concentrating Xe seven to tenfold and Kr three to fivefold from initial feed stream compositions. Because previous isothermal studies of both sorbents have shown that sorbent capacity is proportional to feed gas concentration, it is anticipated that a series of successively smaller HZ-PAN columns will further concentrate and purify the final Kr stream with higher efficiency. It is expected that Xe will be released to atmosphere after desorption. However, it could also be purified further with more AgZ-PAN columns in series. It is recommended that further studies be conducted to determine the maximum practical purity of Kr and Xe achievable utilizing gas adsorption. (A. Welty)

- **[ORNL]** The report for milestone M4NT-18OR030107023, "Evaluate the results of extended duration test of VOG sorbents to support the determination of key engineering parameters," has been completed. This test represents the longest extended VOG test conducted to date by this program. This test ran 38 weeks and achieved iodine loadings of ~40 mg I/g sorbent. The iodine mass transfer zone penetrated at least 10.5 cm into the sorbent beds. There was no indication of sorbent saturation. The mass balance for iodine closed within 2%, which is within the expected combined uncertainty. While this test did not achieve saturation of any portion of the test beds, the data does provide significant information that can be used to extrapolate a potential maximum length of the mass transfer zone under VOG conditions. Under the conditions used in this test, the mass transfer zone could be on the order of 21 cm.
- **[ORNL]** The Level 3 milestone, M3NT-18OR030107024 titled, "Prepare draft report on the design and testing of the integrated iodine scrubber and polishing bed test," has been completed. The draft report summary follows:

  The testing described in this report was intended to provide an evaluation of an integrated system in which bulk iodine is first removed by an aqueous NaOH scrubber with a target iodine DF of > 20. The effluent from the scrubber is then passed through an AgZ sorbent bed to remove residual iodine. The integration of these unit operations was intended to demonstrate an iodine DF of >1000, which would facilitate regulatory compliance with regard to total volatile radionuclide emission from a reprocessing facility. This caustic scrubber system achieved DF's significantly in excess of the target values for both CO_2 and elemental iodine. Only trace amounts of iodine remained to be captured on the polishing bed. (B. Jubin)

- **[ORNL]** An integrated test was completed in July that examined the performance of an iodine removal system that included a caustic scrubber followed by an AgZ polishing bed. In August, a test was conducted with identical test conditions that did not include the caustic scrubber. The performance of the AgZ bed in each scenario will be compared. Results for the scrubber bottoms analysis and sorbent bed have been returned for the first test; analytical results for the second test are pending. 96% of the iodine delivered to the system was recovered in either the scrubber bottoms or the solid sorbent bed; this represents closure of the mass balance within experimental error. The scrubber was very efficient in iodine removal, with only 0.008% of the iodine delivered to the system passing through the scrubber and accumulating on the solid sorbent bed. (B. Jubin)
- **[ORNL]** Milestone M3NT-18OR0301070211 titled, "Complete the initial series of Ru adsorption optimization studies and provide recommended changes to the assumptions used in the analysis of an integrated off-gas system," was completed with the issuance of the technical report. The summary of the report follows:

  The tritium pretreatment process will release a fraction of the ruthenium as volatile ruthenium tetroxide (RuO_4). Tests were conducted to examine the deposition phenomena and provide preliminary information pertinent to an engineering design of a sorption bed to remove RuO_4 from a gas stream (e.g., approximate length of the mass transfer zone and the loading per unit

mass of sorbent). Adsorption media included stainless steel wire mesh (screen) to act as a thin bed sorbent and steel wool packing to act as a deep bed sorbent. Initial tests showed that RuO_4 deposited on a variety of heated surfaces (temperatures > 100°C), including the Teflon O-rings used as spacers between the wire mesh disks, glass spacers, quartz tube, and the metallic sorbents. Deposition at room temperature was very minimal, permitting the use of Teflon tubing for unheated sections of the apparatus. Deposition became very rapid and complete at elevated temperatures (i.e., at 150°C or higher). At a bed temperature of 150°C and carrier gas flowrate of 0.25 slpm through a 1-in. ID quartz tube, penetration of the RuO_4 into the bed varied strongly with the packing density of the steel wool, ranging from 1.5 in. to 6 in. Increasing the bed temperature to 250°C decreased the penetration into the bed to under 0.7 in. In one test an attempt was made to load the sorbents to saturation. This was done by loading the bed with a specific amount of ruthenium, visually observing the depth of deposits on the bed and repeating the sequence four times. The depth of penetration did not change, indicating that deposition only required a heated surface, including a surface already covered with (presumably) RuO_2. (B. Jubin)

- [**ORNL]** Work is underway on the task to determine the impact of variations in NO, NO2 and water concentrations on iodine adsorption rates. A total of five thin bed tests have been completed examining the impacts of water, NO, NO2, and sorbent temperature on the adsorption of methyl iodide by AgZ. Estimated loadings (based on weight measurements) or finalized loadings (based on neutron activation analysis of sorbent iodine content) are found in Table 2 for each test completed. A sixth test is underway. (B. Jubin)

Table 2: NOx-CH3I Test Matrix

Run No	**Iodine Loading (mg I/g sorbent)**	**X_1 Temp (135 or 165°C)**	**X_2 [NO] 0 or 1%**	**X_3 [NO_2] 0 or 1%**	**X_4 Dew Point (-60 or 0°C)**
FY18-006	70	-	-	-	-
FY18-008	30 (est)	+	-	-	+
FY18-009	20 (est)	-	+	-	+
FY18-007	0.4	+	+	-	-
FY18-010	24 (est)	-	-	+	-
		+	-	+	+
FY18-011	In progress	-	+	+	+
		+	+	+	-

- **[ORNL]** Testing for the milestone, "Quantify the potential physisorption on silver-based solvents that was potentially observed in FY-17 VOG testing," has been completed and analysis of solid sorbent samples at ORNL's High Flux Isotope Reactor is pending. (B. Jubin)
- **[ORNL]** The method to capture tritium from Zr recycle off-gas depends greatly whether Cl2 or HCl is used in the zirconium volatilization step. Because the current baseline process uses Cl2, the focus has been on methods to separate 3HCl (or TCl) from Cl2. Solid sorbents including molecular sieves and a potential chemisorption reagent, which may be used in a dry system, have been identified for testing. Another approach to remove the tritium from the cladding by heating it in an inert gas has also been considered. A draft technical report describing the technologies and pre-conceptual design of implementing systems is about 75% complete. The report will also include recommendations for selecting and testing the technologies. (B. Jubin)
- **[PNNL]** A series of experiments were conducted to improve the mechanical stability of MOF materials with various binder concentrations using a previously described wet granulation method. Along with CaSDB MOF, two other prototypical MOFs were examined to gain insights into the

versatility of the wet granulation method. We chose three distinct binders for palletization of MOFs: mesoporous alumina, sucrose, and polyacrylic acid (PAA). Briefly, MOF powder (1.0 g), binder (7.0 or 15.0 wt% for MOF powder), and water were mixed using the custom small pan-type granulator. During the mixing process, water was uniformly sprayed onto the samples to achieve the desired particle growth. Granules with a wide size distribution were produced and sieved to yield pellets 600-850 μm in diameter. Powder X-ray diffraction patterns are presented in Figure 10 below for several of the products. To measure the ability of the dried pellets to remain intact during handling, we vigorously shook ~5 mg of pellets in a 20 mL vial. We compared the attrition rates by measuring the amount of powdered MOF that resulted. As shown in Table 3, the simulated handling method resulted in significant powderization of the CaSDB MOF pellets pressed at 12 MPa compared to pellets with various binder concentrations. Robust particles of CaSDB MOF were formed at high loadings of binder (15 wt%), with <1% of the pellets powderizing with sugar and mesoporous alumina binders. Under the described wet granulation conditions, PAA was ineffective as a binder for CaSDB MOF, as significant amounts of the pellets turned to powder after handling. Mesoporous alumina was found to be a promising binder for NiMOF, however the opposite was true for HKUST-1, as the particles formed via pressure had a lower attrition rate. Powder X-ray diffraction studies confirmed the chemical stability of CaSDB MOF towards the binders and the wet granulation process. There is still lot of work needed to optimize binder concentration without significant loss of adsorption capacity. (P. Thallapally)

Table 3. Attrition rates of the synthesized pellets after simulated handing.

MOF	form	%loss
CaSDB MOF	Pellet (pressed at 12 MPa)	26.4
	Pellet – 7% Al	10.0
	Pellet – 15% Al	0.5
	Pellet – 7% sucrose	3.1
	Pellet – 15% sucrose	0.5
	Pellet – 7% PAA	11.7
	Pellet – 15% PAA	23.9

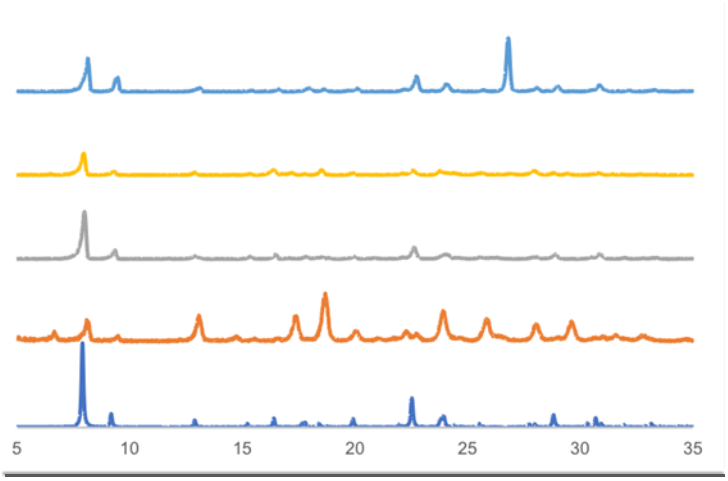

Figure 10. Powder X-ray diffractograms of CaSDB MOF. From bottom to top: simulated pellets of CaSDB MOF obtained from single-crystal data, 15%wt mesoporous alumina, 15%wt sucrose, 15%wt PAA, and 15%wt graphite.

FLOWSHEET DEMONSTRATIONS

- **[PNNL]** The milestone report M3NT-18PN030109016, titled, "CoDCon Project: FY 2018 Status Report," (NTRD-MRWFD-2018-000224) was issued. The work scope in FY 2018 included performing two CoDCon flowsheet tests using 2-cm centrifugal contactors. For both of these tests, U and Pu were extracted from 3 M HNO3 solutions into an organic solvent consisting of 30 vol% TBP dissolved in n-dodecane. The starting U and Pu concentrations in the aqueous phase were approximately 1 M and 15 mM, respectively. The Pu was stripped from the loaded solvent with a U(IV) solution (~50 mM) and the flowsheet conditions were adjusted to allow bleed-over of some U into the Pu-containing product stream. The amount of U accompanying the Pu was monitored in real time using optical spectroscopic techniques coupled with chemometric modeling. Based on the real-time spectroscopic measurement of the U/Pu ratio, adjustments were made to the flow rate of the fresh TBP solvent phase used to scrub U from the aqueous Pu-containing product. This proved to be a very effective way to control the U/Pu mass radio in the product.

  For the first CoDCon flowsheet test, the relative mass fractions of U and Pu in the product were 61% and 39%, respectively. This U/Pu mass ratio of 1.56 was substantially lower than the target value of 2.33 (7/3). This was attributed to the chemometric models incorrectly indicating the presence of U(VI) in the product solution. Nevertheless, the relative Pu mass fraction was maintained within 3% of the mean value throughout the experiment. Adjustments were made to the chemometric model based on the results of the first test to correct the inaccurate results in the real-time analysis of the process solutions.

  During the second CoDCon flowsheet test, the relative amounts of U and Pu in product solution were initially ~80% and 20%, respectively. However, after adjustments to the fresh TBP solvent phase, the target ratio was achieved, and this was maintained over approximately 2.5 h of operation. The final U/Pu nitrate solution contained 29.3% Pu and 70.7% U. This result demonstrated the utility of real-time spectroscopic monitoring in guiding process operations, and also showed that, once steady state is reached, a very stable U/Pu ratio can be maintained. (G. Lumetta)

For more information on Material Recovery and Waste Forms Development contact Terry Todd (208) 526-3365

MPACT Campaign

MANAGEMENT AND INTEGRATION

NTD & Technical Support

- **[LANL]** MPACT NTD & CAM prepared the FY19 MPACT Planning Package information. Reviewed specific activities with Principle Investigators (PIs) and Work Package Managers (WMPs) to develop FY19 budget estimates and milestones. Began preparations for MPACT annual meeting to be held in Washington D.C.

SAFEGUARDS AND SECURITY BY DESIGN - ECHEM

Voltammetry

- **[ANL]** Data analysis of the long-duration test of sensor performance was performed. Extensive statistical examination has confirmed the stability and repeatability of the measurements. Additional testing is taking place in September to automate acquisition and analysis of data from the sensor.
- **[INL]** Cyclic voltammetry (CV) was performed in the Integrated Recycling Test (IRT) oxide reduction furnace (OR). A build up of a deposit was observed early on in the tungsten electrode. In an attempt to sample the deposit, the tungsten electrode was broken off leaving only 2-3 mm extruding from the MgO tube. The deposit left in the furnace was electrochemically removed from the electrode continuing the CVs throughout the month. There are differences in the CVs collected in the lab compared to what is being measured in the IRT OR. Time was also spent analyzing the data and trying to understand what is happening on the working electrodes in an effort to bridge the gap between the lab scale and field testing CV.

Sensor for Measuring Density and Depth of Molten Salt

- **[INL]** Bubbler tubes 1 and 3 became obstructed. The month was spent attempting to clear the tubes, writing the year end report, modifying a height gauge for HFEF use, and preparing for the Fall MPACT meeting. By the end of August, the tubes had not been successfully cleared. The height gauge is nearly ready for use in HFEF (the dip tube needs modified to eliminate salt drop issues).

Microfluidic Sampler

- **[ANL]** Parts for the acrylic prototype of the custom molten salt centrifugal pump were 3-D printed at the Argonne Advanced Photon Source fabrication facility. These parts are being assembled for use in water testing. Additionally, preliminary water testing of the acrylic flow cell droplet generator was carried out. Designs for high temperature pump seals and bearings were investigated.

Electrochemical Sensor

- **[INL]** Uranium sensor testing work was continued in MFC FASB and EDL glovebox. The sensitivity test results have shown promise. The results will be presented at the MPACT Working Group Meeting. SEM analysis was performed in order to examine possible microcrakes in ceramic membrane. It was observed that microcracks did present in U-membrane ion exchanged at 795C. The U membrane made by ion exchange at 750C followed by 800C/10hr annealing was significantly improved. It has better mechanical strength, but still very small microcracks were observed under SEM.

ADVANCED INTEGRATION

Advanced Integration (Methods)

- **[LANL]** Integrated HDND data, new Microcal data, and have begun work on Voltammetry using a standard flow sheet from SSPM.

Advanced Integration (Facility Models)

- **[SNL]** The Molten Salt Reactor Safeguards Model Report has been completed and submitted. A trip to ORNL was used to coordinate MSR safeguards work for next year.

EXPLORATORY RESEARCH / FIELD TESTS

Microcalorimetry

- **[LANL]** Completed M2 milestone report, "Microcalorimeter Gamma Spectrometer Field Testing Readiness“ (M2NT-18LA00106021). The report reviews requirements and instrument status for testing advanced fuel cycle safeguards capabilities through measurement campaigns at LANL and field testing at new locations. The gamma spectrometer that we have developed over the past year by integrating the University of Colorado SLEDGEHAMMER detector assembly with a LANL cryostat and readout system is the first full-scale high-throughput instrument. It represents a major milestone in the development of microcalorimeter technology and is ready for measurement campaigns at LANL. Only minor development is needed for field testing at new locations. Details of measurement campaigns are being planned and will be discussed at the MPACT Working Group Meeting.

In situ Measurement of Pu Content in U/TRU Ingot

- **[INL]** Evaluation on Pu content determined by cooling curve measurements and destructive analysis on the fourth JFCS U/TRU ingot continued. Several U/Pu phase diagrams were investigated for comparison. The results will be presented at Plutonium Futures –The Science 2018 Conference, Sept. 14-18, San Diego, CA. The detailed evaluation and analysis will be included in the year-end report.

For more information on MPACT contact Mike Browne at (505) 665-5056.

Systems Analysis and Integration (SA&I) Campaign

CAMPAIGN MANAGEMENT

- **[ANL, INL]** Presented the Campaign planning information during the FY 2019 Planning Package Meeting held at DOE-HQ, Germantown, August 1-2, 2018. After review comments were received from NE-4, completed the three SA&I Campaign Planning Packages, and had all of them approved by the campaign Federal manager and director.
- **[ANL, BNL, INL, LLNL, ORNL, PNNL, SNL]** Campaign Lab leads/Work Package Managers started working on the Work Packages for FY 2019.

EQUILIBRIUM SYSTEM PERFORMANCE (ESP)

Performance of Fuel Cycle Systems

- **[ANL, BNL, INL, ORNL]** The report entitled "Compendium Report on the Performance Analysis of Innovative Nuclear Energy Systems," by T. K. Kim, et al., was submitted to campaign management. This report is a deliverable in fulfillment of the Level 2 milestone, M2NT-18AN120102011, under the work package "NT-18AN12010201 – Equilibrium System Performance (ESP) - ANL." The report was reviewed by Mr. J. Buelt and Dr. W. Halsey. This milestone is a compendium report on advanced nuclear energy systems and associated fuel cycles that are currently being developed by industries, universities, national laboratories, and foreign entities.
- **[ANL]** Submitted a full paper to the 15th International Exchange Meeting on Actinide and Fission Product Partitioning and Transmutation (15IEMPT). The paper summarized the fuel cycle performance of once-through sustainable sodium-cooled fast reactor.
  - T. K. Kim, et al., "Once-through Sustainable Sodium-cooled Fast Reactor."
- **[ANL]** Reviewed and commented on the report documenting the development of the transmutation library database. Interacted with N. Brown (PSU) to discuss the fairly extensive comments.
- **[INL]** Worked for analyzing the impact of partially loaded LEU fuels within TRU fueled breakeven SFR on the transition of nuclide evolutions and core characteristics particularly focusing on uncontrolled burnup reactivity swing, utilizing the SFR core model developed in the previous month. The analysis also attempted to reduce reactivity swing and excess reactivity while the LEU fuel is loaded to the level equivalent to those of the equilibrium breakeven SFR in order to see how cycle lengths and/or power levels need to be sacrificed without insertion of control elements.
- **[LLNL]** Provided an independent review of the ANL led level-2 milestone report "Compendium Report on the Performance Analysis of Innovative Nuclear Energy Systems" by T. K. Kim, et al (NTRD-FCO-2018-000438).

Economic Analysis Capabilities and Assessments

- **[ANL]** The letter report entitled "Letter Report on the Development and Public Release of the NE-COST Website," by F. Ganda, et al., was submitted to campaign management. This report is the deliverable in fulfillment of Level 3 milestone, M3NT-18AN120102014 under the work package of "NT-18AN12010201– Equilibrium System Performance (ESP) - ANL." The objectives of the NE-COST website are primarily to provide a credible source of information on fuel cycle cost to all the interested stakeholders by providing convenient access to credible source of information on fuel cycle costs and computationally accurate economic quantification of the Levelized Cost of Electricity at Equilibrium (LCAE) − with user selected cost and financial parameters. The website is https://cnpce.ne.anl.gov/.

- **[ANL]** Completed an urgent, high priority request to support the VTR leadership, with an assessment of the expected cost of the VTR reactor using the ACCERT algorithm, for the CD-0 cost estimate. After an early delivery of preliminary cost data through a working excel spreadsheet, the report "VTR preliminary cost estimate with the ACCERT code", by F. Ganda, et al. was completed and delivered to the VTR management. The report explains the approach behind the total estimated costs.
- **[ANL, INL]** Continued the preparation of the Cost Basis Report Milestone, which includes the revision of the module F2D2 on pyroprocessing and remote fabrication based on newly discovered data from KAERI, Korea and from early 1990s cost studies by General Electric, and with a re-organization and restructuring of existing cost data and discussions. Additionally, a dry processes submodule and new cost data for MOX fabrication, both for LWR and for fast reactors, based on newly found bottom-up NASAP studies from the late 1970s, were added.
- **[ANL]** Gathered information to generate a rough order of magnitude cost estimate for extracting Pu from potential wastes.
- **[INL]** Completed the revisions to Module F2/D2 for the Cost Basis Report. This included updating the basis for cost, which included escalating previously reported costs to 2017 USD. Further, drafted a new section for F2/D2, which provides a cost basis for other "dry processes" not previously, such as CARBOX, AIROX, and DUPIC.

Equilibrium System Performance (ESP) Tools Development

- **[SNL]** We continued to make progress on improving our internal processes for data entry and prepared for the annual working group meeting in September.

DEVELOPMENT, DEPLOYMENT AND IMPLEMENTATION ISSUES (DDII)

Technology and System Readiness Assessment (TSRA)

- **[LLNL]** Review of the revision of the Technology and System Readiness Assessment report.

Transition Analysis Studies

- **[ANL, ORNL]** Submitted two full papers to the 15th International Exchange Meeting on Actinide and Fission Product Partitioning and Transmutation (15IEMPT). The papers summarized the core design of fast spectrum molten salt reactor and its fuel cycle performance characteristics.
  - B. Feng, et al., "Core Design and Simulation of a Fast Spectrum Chloride Molten Salt Reactor."
  - E. Hoffman (ANL), B. Betzler (ORNL), et al., "Impact of Technology Characteristics on Transition to a Fast Reactor Fleet."
- **[ANL, INL]** Submitted a full paper to the 15th International Exchange Meeting on Actinide and Fission Product Partitioning and Transmutation (15IEMPT). The paper summarized the infrastructure and material requirements and considerations that impact the transition from the current LWR fleet to an advanced fast reactor fuel cycle.
  - T. Taiwo, et al., "Lesson Learned from Recent Nuclear Fuel Cycle Scenario Studies."
- **[ORNL]** A full paper for IEMPT-15 was completed and is undergoing internal review. This paper discusses modeling a single-stage fast molten salt reactor with ORION. The results from ORION are compared with a SCALE-based reactor physics model to identify any differences. The objective of the paper is to capture the results of the modeling and insights learned regarding MSR analysis and transition, including capabilities of the tools. The results are consistent with those reported in the recent ANL milestone report.

- **[ORNL]** Advice and mentoring continued for the summer intern who was evaluating the fast spectrum MSR fuel cycle analyses. A basis for comparison was formed between the four different systems being simulated and to define the desired outputs and results to extract from the MSR fuel cycle simulations. Future publications are being considered to capture the work by the intern, and to provide him opportunity beyond the work for the Campaign.

Regional and Global Analysis

- **[ANL]** The EDGAR code was used for preliminary nuclear load following economic analysis. In particular, EDGAR allows simulating the possibility of operating PWR units in load-following mode, which depends on the capability of compensating the Xenon-induced reactivity transients by extracting the control rods or by adjusting boron concentration. This model of nuclear load following was applied to assess the economic benefit of operating PWR units in load-following mode in the scenario of large solar penetration, and showed reduction in the electricity production cost is expected by avoiding over-production penalties. The work was summarized in a full paper and submitted to the 6th International Conference on Nuclear and Renewable Energy Resources.
  - N. Stauff, et al., "Economic Impact of Flexible Nuclear Operation Estimated with EDGAR Optimization Code."
- **[PNNL]** Completed and delivered milestone report on the investigation of state Renewable Portfolio Standards (RPS) on US electricity generation. The report investigates the long-term impact of RPS on total renewable and nonrenewable energy shares and nuclear energy generation using the GCAM-USA model.

For more information on Fuel Cycle Options contact Temitope Taiwo (630) 252-1387.

Joint Fuel Cycle Study Activities

- Process experiments were performed with two separate batches of interim spent LWR fuel in HFEF. Vacuum distillation of residual salt was completed on the first batch.
- INL hosted a delegation from the Korean Ministry of Science and Information Technology (MSIT) as a part of a JFCS program review.
- The JFCS Phase III CRADA was signed by INL, ANL, and KAERI.
- Analytical results were received for a number of prior ER Salt and U/TRU material sampling points.

For more information on Joint Fuel Cycle Studies Activities contact Ken Marsden (208) 533-7864.

AFCI-HQ Program Support

UNIVERSITY PROGRAMS

Site: University Research Alliance at West Texas A&M University in Canyon TX, and the following universities: University of Michigan, University of Tennessee, University of California at Berkeley, Texas A&M University, Vanderbilt University, University of Idaho, Oregon State University, Kansas State University, Northwestern University, University of Nevada at Las Vegas, Clemson University, Rensselaer Polytechnic Institute, Purdue University, Georgetown University, Virginia Commonwealth University, Florida International University, and other universities.

Universities engaged in Nuclear Technology research via URA programs since 2001:

Boise State University
Boston College
Clemson University
Colorado School of Mines
Georgia Institute of Technology
Georgetown University
Idaho State University
Florida International University
Florida State University
Kansas State University
Massachusetts Institute of Technology
Missouri University of Science and Technology
North Carolina State University
Northern Illinois University
Northwestern University
Ohio State University
Oregon State University
Pennsylvania State University
Purdue University
Rensselaer Polytechnic Institute
Rutgers University
Texas A&M University
University of Arkansas
University of California at Berkeley
University of California at Santa Barbara
University of Chicago
University of Cincinnati
University of Florida
University of Idaho
University of Illinois at Urbana-Champaign
University of Michigan
University of Missouri
University of Nevada at Las Vegas
University of New Mexico
University of North Texas
University of Notre Dame
University of Ohio
University of South Carolina
University of Tennessee at Knoxville
University of Texas at Austin
University of Virginia
University of Wisconsin
Vanderbilt University
Virginia Commonwealth University
Washington State University

INNOVATIONS IN NUCLEAR TECHNOLOGY R&D AWARDS

Summary Report

- University Research Alliance distributed press releases on behalf of the 2018 Innovations Awards winners. Winners' university department heads, advisors, and newspapers are among those who are formally notified of their achievement.
- University Research Alliance provided information to the First Place Innovations Awards winners and worked with the award winners and the American Nuclear Society on the Innovations in Nuclear Technology R&D Awards special session to be held at the ANS Winter Meeting in November.
- University Research Alliance continued to update the Innovations Awards announcement distribution list in anticipation of the 2019 Innovations Awards.

- ***For more information on the University Research Alliance contact Cathy Dixon (806) 651-3401.***